Optimal Ventilation Control in Complex Urban Tunnels with Multi-Point Pollutant Discharge

Center for Transportation, Environment, and Community Health
Final Report

by
Zhen Tan, H. Oliver Gao

October 31, 2017

DISCLAIMER

The contents of this report reflect the views of the authors, who are responsible for the facts and the accuracy of the information presented herein. This document is disseminated in the interest of information exchange. The report is funded, partially or entirely, by a grant from the U.S. Department of Transportation's University Transportation Centers Program. However, the U.S. Government assumes no liability for the contents or use thereof.

TECHNICAL REPORT STANDARD TITLE PAGE

1. Report No.	2.Government Accession No.	3. Recipient's Catalog No.
4. Title and Subtitle Optimal Ventilation Control in Complex Urban Tunnels with Multi-Point Pollutant Discharge		5. Report Date October 2017 6. Performing Organization Code
7. Author(s) Zhen Tan (ORCID ID 0000-0003-1711-3557) H. Oliver Gao (ORCID ID 0000-0002-7861-9634)		8. Performing Organization Report No.
9. Performing Organization Name and Address School of Civil and Environmental Engineering Cornell University Ithaca, NY 14853		10. Work Unit No. 11. Contract or Grant No. 69A3551747119
12. Sponsoring Agency Name and Address U.S. Department of Transportation 1200 New Jersey Avenue, SE Washington, DC 20590		13. Type of Report and Period Covered Final Report 14. Sponsoring Agency Code US-DOT

15. Supplementary Notes

16. Abstract

We propose an optimal ventilation control model for complex urban vehicular tunnels with distributed pollutant discharge points. The control problem is formulated as a nonlinear integer program that aims to minimize ventilation energy cost while meeting multiple air quality control requirements inside the tunnel and at discharge points. Based on the steady-state solutions to tunnel aerodynamics equations, we propose a reduced form model for air velocities as explicit functions of ventilation decision variables and traffic density. A compact parameterization of this model helps to show that tunnel airflows can be estimated using standard linear regression techniques. The steady-state pollutant dispersion model is then incorporated for the derivation of optimal pollutant discharge control strategies. A case study of a new urban tunnel in Hangzhou, China demonstrates that the scheduling of fan operations based on the proposed optimization model can effectively achieve different air quality control objectives under varying traffic intensity.

17. Key Words	18. Distribution Statement
air quality, ventilation control, urban tunnels, nonlinear programming	Public Access as well as a resulting journal manuscript submitted, based on which this report is developed.

19. Security Classif (of this report)	20. Security Classif. (of this page)	21. No of Pages	22. Price
Unclassified	Unclassified		

Form DOT F 1700.7 (8-69)

Optimal Ventilation Control in Complex Urban Tunnels with Multi-Point Pollutant Discharge

Zhen Tan and H. Oliver Gao

***Abstract*— We propose an optimal ventilation control model for complex urban vehicular tunnels with distributed pollutant discharge points. The control problem is formulated as a nonlinear integer program that aims to minimize ventilation energy cost while meeting multiple air quality control requirements inside the tunnel and at discharge points. Based on the steady-state solutions to tunnel aerodynamics equations, we propose a reduced form model for air velocities as explicit functions of ventilation decision variables and traffic density. A compact parameterization of this model helps to show that tunnel airflows can be estimated using standard linear regression techniques. The steady-state pollutant dispersion model is then incorporated for the derivation of optimal pollutant discharge control strategies. A case study of a new urban tunnel in Hangzhou, China demonstrates that the scheduling of fan operations based on the proposed optimization model can effectively achieve different air quality control objectives under varying traffic intensity.**

***Index Terms*—** air quality, ventilation control, urban tunnels, nonlinear programming

I. Introduction

TUNNELS are an important component of the modern transportation infrastructure system, especially in and near urban areas like central business districts (CBD) where transportation has to compete with commercial and residential activities for limited urban space [1]. Due to various topographic and functional complexity within a road network, tunnel branches/ramps are necessary to connect the main tunnels to the rest of the transportation network. For example, the popular urban traffic link tunnels (UTLT) have a main tunnel with several adjoining ramp tunnels connecting accesses to various buildings [2]. Several cities have started to move surface road traffic to below ground (e.g., tunnel A86 in Paris and tunnel M30 in Madrid) [1] with multiple ramp tunnels linking to the surface transportation network. The airflow interactions in different tunnel branches lead to complicated aerodynamics in the tunnel [2][3], which in turn affect pollutant dispersion in the tunnel. In the meantime, the large volume of traffic (hence emissions) together with the quasi-closed space in a tunnel easily makes it a hotspot with elevated air pollution for travelers inside the tunnel. Emission discharges at the tunnel portals also constitute a major concentrated source of emissions that present adverse impacts to the public nearby. For mitigation, tunnel ventilation systems are designed to help distribute and discharge emissions at multiple points (e.g., through tunnel upper vents) [4]. Emission rates at these discharging points are subject to emission standards for ambient air quality control. Effective design and operation of tunnel ventilation and emission discharge, adapted to complex tunnel geometry and operations, is therefore critical for meeting various air quality and emission control requirements. Most of the tunnels are equipped with typical longitudinal ventilation system due to its efficiency and relatively low cost [5]. The longitudinal tunnel ventilation system is designed and operated to fulfill two objectives: 1) maintaining the concentrations of criteria pollutants such as carbon monoxide (CO), nitrogen oxides (NO_x), and $PM_{2.5}$ below admissible standards for health and visibility purposes; and 2) reducing energy cost of jet-fan operations [6] [7]. These two aspects are also important factors for consideration in multi-point pollutant discharge control in complex tunnels.

Existing research of tunnel pollution control has mostly focused on controlling maximum pollutant concentration inside single-exit tunnels [6]-[11]. Even though some recent efforts were made to study tunnel ventilation with upper vents and complex tunnels with single discharge point, there remains a significant knowledge gap for successful ventilation control in complex urban tunnels with distributed multi-discharge points. Study [12] adopted the one dimensional aerodynamics model to analyze airflow through multiple tunnel upper vents under natural ventilation. Their results suggest that enlarging the individual vents and decreasing the spacing between vents are good options for tunnel pollution control. Scaled experimental tests and numerical simulation were conducted in [13] to analyze the airflow in a traffic tunnel that has multiple natural vents. Alternating flows between air intake and exhaust discharge were observed in the natural vents under continuously moving traffic. A recent study [14] also used the one-dimensional tunnel airflow model and numerical analysis to investigate smoke control by combining longitudinal ventilation with natural roof venting, which was found to be effective for smoke control under proper combination of vents spacing and jet fan operation intensity. Considering only natural upper venting, however, these studies do not include active mechanical ventilation in upper vents that is often used in urban tunnels with heavy traffic [2]. Active control of airflows through upper vents can improve efficiency in ventilation design. In real-world applications, ventilation in tunnels such as the Taihu tunnel [4] is designed with upper vents that can be operated for air extraction or supplement to achieve better control of the tunnel environment.

As for optimal tunnel ventilation control (in terms of energy efficiency), studies [15][16] proposed an tunnel ventilation control optimization method using linear programming. Taking longitudinal air velocity inside the tunnel as an affine function

of the fan power, these studies were able to use the steady state pollutant dispersion model to a simulated loop tunnel for ventilation control objectives discussed earlier. However, the model considers only the in-tunnel pollutant concentration control and assumes that polluted air in the tunnel is discharged at only one ventilation shaft. As we will show later, when multiple discharging points are considered, the ventilation control problem can no longer be formulated via linear programming even simple affine relationship between fan intensity and velocity is employed. Hence, a new control model addressing ventilation needs for real world tunnels with multiple discharge points is necessary. In [3] the Subway Environment Simulation Program (SES) software [17] was used for the calculation of ventilation intensity for pollutant discharge control in urban tunnels with multiple ramps. The study, however, did not consider energy efficiency in fan operation. Some recent studies (e.g., [7]) started analyzing ventilation strategy of urban traffic link tunnels for smoke control under fire hazards. A static optimization model for vents layout design of complex tunnels is also proposed [18]. Nonetheless, optimal ventilation fan control in multi-vent tunnels for air quality management has not been well explored.

In this study we propose an optimization model for energy-efficient ventilation and air quality control in complex urban tunnels with multi-discharge points. Using a novel reduced form of quantitative analytics for ventilation control and parameter estimation, we develop a nonlinear integer programming model that can accommodate various air quality management constraints.

II. System Modeling

A. System Decomposition

The ventilation and pollutant discharge system in a tunnel can be decomposed into subsystems according to the functional and spatial organization [12]. Functionally, a tunnel system consists mainly of three subsystems: traffic, ventilation, and pollutant emission. Traffic, the source of emissions in the tunnel, is subject to the effect of various transportation factors (e.g., traffic flow density, speed, tunnel throughput and capacity, etc.) that can be described using traffic flow models. Ventilation, usually the air-flow field characterized by aerodynamics models, is the result of the combined impacts of jet-fan operations and running vehicles ("piston effect"). This is the major driving force for vehicular emissions in the tunnel to be dispersed and discharged. Pollutant release (or emission) at discharge points is affected jointly by tunnel traffic and ventilation. The source strength of pollutant emission depends on traffic conditions such as traffic intensity, vehicular mix, and vehicle emission factors. The time-space distribution of pollutant concentration is influenced by ventilation and dispersion in the tunnel.

Spatially, a tunnel can be divided into connected segments for ventilation analysis by access points of ramps and upper vents along the mainline. The whole tunnel system with multiple discharge points can be modeled as an aerodynamics system within a serial-branch structure. In this study we focus on one-way traffic tunnels that have multiple branches. It is common to use one separate channel for each traffic direction in urban tunnels, and the models we developed can be extended to the two-way traffic case by considering the effect of vehicle motion in the other direction [19][20]. Techniques in [7] can be used to convert a looped tunnel to a branched one.

Fig.1 shows an example of a one-way traffic tunnel with multiple ramps and pollutant discharge vents. Tunnel segments are indexed by $i \in I = \{1, 2, \ldots, n + m\}$. Without loss of generality, we assume that only the mainline tunnel has upper vents, and each tunnel ramp is treated as one tunnel segment. The mainline tunnel segments are numbered from $i = 1$ to n, in the order from the entrance to the exit, and the ramp segments are numbered from $n + 1$ to $n + m$ along the direction of traffic. This implies that the total number of upper vents along the mainline ceiling is $n - m - 1$. Each upper vent is equipped with either extraction or supplement fans. Pollutants can be released at all discharge points (i.e., tunnel and ramp exits as well as air extraction vents), within regulated emission rate limits.

For modeling purpose, we label on-ramp and off-ramp segments separately by index sets I_{on} and I_{off}, respectively. For any ramp segment $i \in I_{on} \cup I_{off}$, we use h_i and $h_i + 1$ to denote the upstream and downstream mainline tunnel segments that connects at the access point of the ramp segment i (i.e., the access point of the ramp is the division point of mainline segments h_i and $h_i + 1$) . We also define $h_0 = 0$.

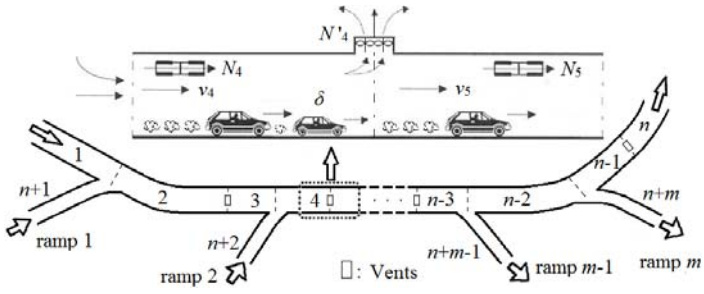

Fig. 1. Complex urban tunnel system

B. Ventilation Control Input, Disturbance, State and Output Variables

The longitudinal mechanical ventilation in a tunnel is mainly controlled by the jet fans installed along the tunnel ceiling. Let I_J be the index set of tunnel segments equipped with jet fans. In addition, distributed upper vents along the tunnel also affect the ventilation and pollutant discharge. Each upper vent can be used either for air extraction or supplement; we use I_{VE} (or I_{VS}) to denote the index set of tunnel segments that have upper vents for air extraction (or supplement) located at their ending points;. So if $i \in I_V = I_{VE} \cup I_{VS}$, then an upper vent is the division point of segments i and $i + 1$. Each vent is designed with a number of axial fans, each with a rate flow of Q_0 (m^3/s). For optimal performance of tunnel ventilation and pollutant discharge, the control system can adjust the number of jet-fans running in the segment, N_i ($i \in I_J$) and the number of axial fans running at each upper vents, N'_i ($i \in I_V$). So N_i ($i \in I_J$) and N'_i ($i \in I_V$) are the control variables in tunnel ventilation.

We take traffic intensity as measured disturbance. Let I_S be the index set of the tunnel segments that has traffic sensors. We can use the normalized traffic volume in tunnel segment ($i \in I_S$), which is a dimensionless scalar δ_i (called "*traffic intensity*") obtained by dividing the real traffic volume q^t_i (veh/h) by its predetermined base level $q^0_i > 0$ (veh/h). Traffic intensity in all

segments is encoded by vector $\boldsymbol{\delta} = \{\delta_i, i \in I\}$. Other factors such as traffic speed, fleet mix, boundary atmospheric turbulence are modeled as unmeasured disturbances.

Airflow in the tunnel is the outcome of the combined effects of moving traffic, running jet fans inside the tunnel, and axial fans at the vents. Let v_i be the average longitudinal air velocity (m/s) in tunnel segment i, we consider vector $\boldsymbol{v} = \{v_i, i \in I\}$ as the system state variable, which governs the pollutant dispersion in the tunnel.

The performance measures of concern in tunnel ventilation control include concentrations of various air pollutant p in all tunnel segments, $c^p{}_i$ (mg/m^3, "mg" stands for milligram), and emission rates at the discharge points in segments $i \in I_V \cup I_E$ for different air pollutant p, $Q^p{}_i$ (mg/s). Let I_E denote the index set of all the tunnel segments with exiting traffic (i.e., mainline exit segment $i = n$ and all the off-ramps). These performance measures (e.g., $c^p{}_i$ and $Q^p{}_i$) are required to be maintained below certain limits for air quality control purpose.

In the practice of tunnel ventilation control, ventilating fans are not expected to be switched on and off more often than once every 10 minutes for lifetime saving of the fans. The airflow in a tunnel cannot respond to fan changes faster than such a frequency either [15]. In addition, traffic condition does not notably change over 10-minute time intervals [15] [16]. Considering these facts, a static discrete-time control model is proposed in this study based on steady-state aerodynamics modeling and control for 10-min ventilation control intervals Considering that urban tunnels are generally not too long, it is reasonable to assume, for modeling purpose, that

Assumption 1: The control interval covers the longest travel time of a vehicle through the tunnel.

C. Basic Traffic Intensity and Air Velocity Variables

We use Π^t to denote all the subsets of tunnel segment indices that satisfy the following condition: If subset $I_1 \in \Pi^t$, then during any control interval, traffic intensities in tunnel segments $\{\delta_i, i \in I_1\}$ are linearly independent, while traffic intensities in other tunnel segments δ_i ($I \in I \setminus I_1$) are linear combinations of $\{\delta_i, i \in I_1\}$. We call $\{\delta_i, i \in I_1\}$ the basic traffic intensity variables. Π^a is defined similarly as the indexing set for basic air velocity variables in certain tunnel segments. We have a simple observation:

Lemma 1: Under *Assumption 1*, we have (i) $\Pi^t = \Pi^a$ given the control input N'_i ($i \in I_V$); (ii) A set I_B is in Π^t if and only if it contains for each $s = 1, \ldots, m$, one element in two of the three sets $\{n + s\}$, $\{h_{s-1} + 1, h_{s-1} + 2, \ldots, h_s\}$, $\{h_s, h_s + 1, \ldots, h_{s+1}\}$, and no element from the third set.

Proof: This follows readily from the way how we divide the tunnel into segments and the flow conservation condition. Specifically, define $q^a{}_i = S_i v_i$ as the air flow rate (m^3/s) in tunnel segment i, where S_i is the cross sectional area of tunnel segment i (m^2). By flow conservation, during a control interval k (recall that *Assumption 1* implies the control interval covers at least as long as the longest travel time of a vehicle through the tunnel), we have:

$$\begin{cases} q^t_{h_i}(k) = q^t_{h_{i+1}}(k) - q^t_i(k),\ q^a_{h_i}(k) = q^a_{h_{i+1}}(k) - q^a_i(k), & \forall i \in I_{\text{on}}, \\ q^t_{h_i}(k) = q^t_{h_{i+1}}(k) + q^t_i(k),\ q^a_{h_i}(k) = q^a_{h_{i+1}}(k) + q^a_i(k), & \forall i \in I_{\text{off}}, \\ q^t_i(k) = q^t_{i+1}(k),\ q^t_{i+1}(k) = q^t_i(k) + Q_0 N'_i(k), & \forall i \in I_{VS}, \\ q^t_i(k) = q^t_{i+1}(k),\ q^t_{i+1}(k) = q^t_i(k) - Q_0 N'_i(k), & \forall i \in I_{VE}. \end{cases} \quad (1)$$

Denoting vectors $\boldsymbol{q}^t = \{q^t{}_i, i \in I\}$, $\boldsymbol{q}^a = \{q^a{}_i, i \in I\}$, we can write linear equations (1) in the matrix form $\boldsymbol{A}\boldsymbol{q}^t = \boldsymbol{0}$ and $\boldsymbol{A}\boldsymbol{q}^a = \boldsymbol{b}$ for proper matrix $\boldsymbol{A} \in \mathbb{R}^{(n-1)\times(n+m)}$ with full row rank and vector $\boldsymbol{b} \in \mathbb{R}^{(n+m+1)}$ (noting that $|I_{on}| + |I_{off}| = m$, $|I_V| = n - m - 1$, $|I| = n + m$).

We can reorganize the columns of $\boldsymbol{A}$ as $\boldsymbol{A} = [\boldsymbol{A}_B, \boldsymbol{A}_N]$ such that $\boldsymbol{A}_N$ has full column rank, and $\boldsymbol{q}^t$ and $\boldsymbol{q}^a$ can be partitioned accordingly as $\boldsymbol{q}^t = [\boldsymbol{q}^t{}_B{}^{\mathrm{T}}, \boldsymbol{q}^t{}_N{}^{\mathrm{T}}]^{\mathrm{T}}$ and $\boldsymbol{q}^a = [\boldsymbol{q}^a{}_B{}^{\mathrm{T}}, \boldsymbol{q}^a{}_N{}^{\mathrm{T}}]^{\mathrm{T}}$. Then $\boldsymbol{q}^t{}_N = -\boldsymbol{A}_N{}^{-1}\boldsymbol{A}_B\boldsymbol{q}^t{}_B$ and $\boldsymbol{q}^a{}_N = \boldsymbol{A}_N{}^{-1}(\boldsymbol{b} - \boldsymbol{A}_B\boldsymbol{q}^a{}_B)$. I_B consists of all the column indices of $\boldsymbol{A}_B$ that satisfy the above partition. Since for each tunnel segment $i \in I$, $\delta_i = q^t{}_i/q^0{}_i$ and $v_i = q^a{}_i/S_i$, by definition of Π^t and Π^a we know the set of all such i's is both Π^t and Π^a, so (i) is true.

For the proof of (ii), we notice that the above equations in (1) imply that for each $s = 1, \ldots, m$, knowing one q^t variable in each of any two of the three sets $\{n + s\}$, $\{h_{s-1} + 1, h_{s-1} + 2, \ldots, h_s\}$, $\{h_s, h_s + 1, \ldots, h_{s+1}\}$ is necessary and sufficient to determine all the q^t variables in these three sets. Note that the union of these three sets over all $s = 1, \ldots, m$ is I; and the third set for s is just the second set for $s + 1$, so we have the result. ■

Let $I_B \in \Pi^t$ contain the indices of the segments that has basic traffic intensity variables. Then $|I_B| = m + 1$ and *Lemma 1* imply $\{v_i, i \in I_B\}$ are also basic air velocity variables. Let $I_N = I \setminus I_B$ contain the indices of segments with non-basic air velocity/traffic intensity variables. The objective of this indices split is to build a model that focuses on the base decision variables in segment $i \in I_B$. In particular, our analysis focuses on the basic velocity variables $\boldsymbol{v}_B = \{v_i, i \in I_B\}$.

Remark 1: A standard approach to finding an index set $I_B \in \Pi^t$ is by QR factorization to first find any $(n - 1)$ linearly independent columns in matrix $\boldsymbol{A}$, I_B consists of the indices of the rest of the columns in $\boldsymbol{A}$. In the current application, however, it is easier to do this due to *Lamma 1*. For example, a simple choice can be $I_B = \{1, n + 1, n + 2, \ldots, n + m\} \in \Pi^t$, i.e., the tunnel segments corresponding to mainline entrance, on-ramp entrances and off-ramp exits, where traffic volume is usually measured in practice.

Assumption 2: $I_S \in \Pi^t$.

This assumption states that for any modeling time interval, the traffic intensity in any tunnel segment $i \in I$ is available by measurements $\{\delta_i, i \in I_S\}$ during the same time interval. As will be clear later, this assumption facilitates the incorporation of traffic intensity and its effect in the tunnel ventilation control model. In practice, traffic sensors are (or can be) deployed for real-time monitoring. We also choose $I_B = I_S \in \Pi^t$ for the convenience of aerodynamics modeling below.

D. Steady-State Aerodynamics Model

The airflow inside a typical serial-parallel tunnel system can be characterized by a group of aerodynamic equations that integrate flow continuity conditions and pressure balance conditions. The serial dimension of air movements in a tunnel, modeled according to flow continuity conditions, considers tunnel air flow in and between the longitudinal mainline tunnel segments (divided by ramps). The parallel dimension of air

movements in a tunnel captures the behavior of air flux across boundaries between tunnel facilities (e.g., mainline and ramps), which can be described based on pressure balance conditions. Specifically, modeling of aerodynamics in a ventilated tunnel system includes 3 steps: 1) establishing force balance equation for each tunnel segment; 2) eliminating segment boundary pressure variables based on pressure balance conditions; and 3) eliminating non-basic air velocity variables v_i, $i \in I_N$ using flow conservation conditions. This leads to a quadratic equation set, which consists of the steady-state ordinary differential equations (ODE) in terms of the basic air velocity v_i, $i \in I_B$. More details of in-tunnel aerodynamics modeling are provided in the Appendix. Here we present the resulting general form of the multivariate quadratic equations with respect to $\boldsymbol{v}_B$:

$$\begin{cases} \boldsymbol{v}_B^{\mathrm{T}} \boldsymbol{\Lambda}_1 \boldsymbol{v}_B + \boldsymbol{\eta}_1^{\mathrm{T}} \boldsymbol{v}_B + \omega_1 = 0, \\ \boldsymbol{v}_B^{\mathrm{T}} \boldsymbol{\Lambda}_2 \boldsymbol{v}_B + \boldsymbol{\eta}_2^{T} \boldsymbol{v}_B + \omega_2 = 0, \\ \vdots \\ \boldsymbol{v}_B^{\mathrm{T}} \boldsymbol{\Lambda}_{m+1} \boldsymbol{v}_B + \boldsymbol{\eta}_{m+1}^{\mathrm{T}} \boldsymbol{v}_B + \omega_{m+1} = 0, \end{cases} \tag{2}$$

where $\boldsymbol{\Lambda}_1, \ldots, \boldsymbol{\Lambda}_{m+1} \in \mathbb{R}^{(m+1)\times(m+1)}$ are symmetric matrices, and the values of model coefficients/parameters $\boldsymbol{\eta}_1, \ldots, \boldsymbol{\eta}_{m+1} \in \mathbb{R}^{(m+1)}$, $\omega_1, \ldots, \omega_{m+1} \in \mathbb{R}$ are defined in (A6) in the Appendix. As discussed in the Appendix, we note that $\boldsymbol{\Lambda}_1, \ldots, \boldsymbol{\Lambda}_{m+1}$, $\boldsymbol{\eta}_1, \ldots, \boldsymbol{\eta}_{m+1}$ and $\omega_1, \ldots, \omega_{m+1}$ all depend on and hence can be derived as functions of the ventilation control variables N_i, $i \in I_J$ and N'_i, $i \in I_V$, as well as the traffic intensity $\boldsymbol{\delta}$.

The relationships between the decision variables N_i, $i \in I_J$ (number of running fans in segment i), N'_i, $i \in I_V$ (number of running axial fans at the upper vents in segment i) and the basic tunnel air velocity variables v_i ($i \in I_B$) are fundamental for ventilation control modeling. It is impractical to derive an exact explicit analytical form for this due to complex aerodynamic equations and the coupled effects among different tunnel segments (as seen in the derivation in the Appendix). Empirically, we observe that these relationships can be well approximated by an affine function by solving equation set (2) numerically with various settings of N_i ($i \in I_J$), and N'_i ($i \in I_V$) for given traffic intensity (e.g., results in Fig. 4 in Section IV for a typical tunnel). Such approximation can also be justified according to studies [15][16]: the authors confirmed that the effect of the operating power for ventilation fans on air velocity inside the tunnel segment can be modelled as an affine function based on simulations and measurements in different tunnels. Since fan operating power is proportional to the number of fans N_i at similar jet speed, in-tunnel air velocity v_i can be modeled as an affine function of N_i in our case. In addition, air supplement or extraction flow through upper vents conforms to flow continuity conditions that consists of simple additions, hence we can write the following steady-state airflow equation to approximate the effect of ventilation control variables on the basic flow velocity variables v_i ($i \in I_B$):

$$v_i \approx \sum_{j \in I_J} \alpha_{ij} N_j + \sum_{k \in I_V} \beta_{ik} N'_k + \gamma_i, \tag{3a}$$

where α_{ij} and β_{ik} are linearization coefficients (m/s). α_{ij} represents the marginal contribution of one extra running jet-fan in segment j to the air velocity in segment i; β_{ik} represents the contribution of one additional running axial fan at an upper vent in segment k to the air velocity in segment i; and γ_i is the intercept for segment i (m/s). These parameters α_{ij}, β_{ik} and γ_i can be estimated using linear regression on results from solving (2) with different fan input settings.

Based on flow conservation conditions (1), one notes that the non-basic velocity variables v_i ($i \in I_N$) can be written as linear combinations of the basic velocity variables and the number of running axial fans at the upper vents:

$$v_i = \sum_{j \in I_B} \lambda_{ij} v_j + \sum_{k \in I_V} \mu_{ik} N'_k, \quad \forall i \in I_N, \tag{3b}$$

where λ_{ij} is dimensionless and μ_{il} has unit in m/s. So v_i, $i \in I_N$ can also be approximated by affine functions of N_j ($j \in I_J$) and N'_k ($k \in I_V$), like in (3a). Hence (3a) can actually be generic to characterize all v_i ($i \in I$). Moreover, the linearization parameters in (3a) may vary across different traffic intensity $\boldsymbol{\delta}$ (the main disturbance in the system), we therefore modify (3a) slightly to (4) below to explicitly account for the effect of traffic intensity:

$$v_i \approx \sum_{k \in I_J} \alpha_{ij}(\boldsymbol{\delta}) N_{jk} + \sum_{k \in I_V} \beta_{ik}(\boldsymbol{\delta}) N'_l + \gamma_i(\boldsymbol{\delta}). \tag{4}$$

Note that (4) distinguishes our model from those proposed in earlier studies (e.g., [15]) in that it explicitly models the variation of key model parameters in response to changes in traffic condition. This improves model fidelity and control performance. Specific functions for $\alpha_{ij}(\boldsymbol{\delta})$, $\beta_{ik}(\boldsymbol{\delta})$, and $\gamma_i(\boldsymbol{\delta})$ can be calibrated offline empirically based on the numerical solutions of (2) under various $\boldsymbol{\delta}$ values. We discuss the choice of parameterization for $\alpha_{ik}(\boldsymbol{\delta})$, $\beta_{il}(\boldsymbol{\delta})$, and $\gamma_i(\boldsymbol{\delta})$ in more details in Section III. The advantage of (4) comes from the affine relationship in (3a) modeled under different traffic intensity [16][21]. Since traffic intensity $\boldsymbol{\delta}_B = \{\delta_i, i \in I_B = I_S\}$ can be measured real-time, such direct quantitative models linking traffic and airflow data will prove useful for the design of optimal ventilation control (see Section III). To reduce the number of model parameters without hampering model precision, we make the following assumption (which will be verified true for typical tunnel conditions).

Assumption 3: Model coefficients α_{ik}, β_{il}, and γ_i in (4) of air velocity in tunnel segment i are affected only by the traffic intensity in segment i and that in adjacent segments.

In other words, we only need to consider the effects of traffic intensity in nearby segments on the airflow in a tunnel segment. . Specifically, we have the following observation:

Lemma 2: With *Assumption 3* above, for each tunnel segment $i \in I_B \in \Pi'$, the coefficients α_{ij} ($j \in I_J$), β_{ik} ($k \in I_V$), and γ_i in airflow equation (4) depend on traffic intensity vector $\boldsymbol{\delta}$ through linear mapping $\boldsymbol{T}_i \boldsymbol{\delta}_B$, $\boldsymbol{T}_i \in \mathbb{R}^{3\times(m+1)}$.

Proof: This follows directly from the definition of Π'. ■

E. Steady-State Air Pollutant Dispersion Model

The distribution of air pollutant concentration inside a longitudinally ventilated tunnel can be described by one-dimensional diffusion-advection equations [7][10][15]. Pollutant deposition (the sink term in a diffusion-advection equation) is usually neglected due to its limited effect on the dispersion and movement of gaseous pollutants inside the tunnel [22]. As a result, for each tunnel segment we have:

$$\frac{\partial c_i^p}{\partial t} = \frac{\partial}{\partial x_i}\left(k_x \frac{\partial c_i^p}{\partial x_i}\right) - v_i \frac{\partial c_i^p}{\partial x_i} + q_i^p, \tag{5}$$

where $c^p{}_i$ is concentration of pollutant p in segment i (mg/m^3), x_i is the distance from the starting point of segment i (m), k_x is the longitudinal diffusion coefficient (m^{-2}), $q^p{}_i$ is the emission rate

of pollutant p (mg/m^3/s), which is the emission from running vehicles in tunnel segment i. Given that advection and source emissions generally dominate the distribution of pollutant concentrations in the tunnel [22], (5) can be further simplified by dropping the diffusion term. The steady-state solution to the simplified tunnel diffusion-advection equation then takes the simple form: $c^p{}_i(x_i) = c^p{}_{0i} + q^p{}_i x_i / v_i$, which implies that the steady-state pollutant concentration increases linearly with distance x_i from the upstream end and achieves its maximum value at the downstream end of the tunnel segment (when $x_i = L_i$ is the length of the tunnel segment) [22]:

$$c^p_{\max i} = c^p_i(L_i) = c^p_{0i} + \frac{q^p_i L_i}{v_i}, \tag{6}$$

where $c^p{}_{\max\ i}$ is the maximum air pollutant concentration in tunnel segment i (mg/m^3). $c^p{}_{0i}$ is the concentration of pollutant p at the upstream end of segment i (mg/m^3): it depends on the pollution level, air supplements, and ramp accesses in the upstream segments. $c^p{}_{0i}$ can be determined for different types of tunnel segments as discussed below.

For the mainline entrance segment and the on-ramp segments that are inlets of traffic and are connected directly to the open air outside of the tunnel, we have the boundary condition for these tunnel segments:

$$c^p_{0i} = c^p_{amb}, \quad (i = 1 \text{ or } i \in I_{on}). \tag{7a}$$

where $c^p{}_{amb}$ is the ambient pollutant concentration outside the tunnel (mg/m^3), which depends on surrounding air quality conditions.

For two adjacent mainline segments divided by an air extraction vent or an off-ramp access point,

$$c^p_{0i+1} = c^p_{\max i}, \ (i \in I_{VE} \text{ or } i = h_j, j \in I_{off}). \tag{7b}$$

For two adjacent mainline segments divided by an air supplement vent, by continuous conditions and conservation of mass [12],

$$c^p_{0i+1} = \frac{v_i S_i c^p_{\max i} + Q_0 N'_i\, c^p_{amb}}{v_i S_i + Q_0 N'_i}, \quad (i \in I_{VS}). \tag{7c}$$

For two adjacent mainline segments divided by the access point of an on-ramp,

$$c^p_{0i+1} = \frac{v_i S_i c^p_{\max i} + v_{n+j} S_{n+j} c^p_{\max n+j}}{v_i S_i + v_{n+j} S_{n+j}}, \ (i = h_j, j \in I_{on}). \tag{7d}$$

Based on the pollutant concentration distribution, we can derive pollutant discharge rate at tunnel discharge points. For tunnel exit and off-ramps, pollutant discharge rate is:

$$Q^p{}_i = v_i S_i c_{\max i}, \ (i = n \text{ or } i \in I_{off}). \tag{8a}$$

For upper vents with air extraction in a tunnel segment,

$$Q^p_i = Q_0 N'_i\, c_{\max i}, \ (i \in I_{VE}). \tag{8b}$$

III. Optimal Ventilation Control

A. System Inputs/Control and State

As shown in (2), fan operations in a tunnel segment or at a vent will affect air velocity in every segment of the tunnel, but with varying magnitudes of effect for different segments. This is an important aspect to consider for the design of ventilation control. Further, the effect of ventilation fans on air flow is influenced by traffic intensity. For practical control purpose, we need to calibrate this dependency quantitatively.

Define $\boldsymbol{u}(k) = [N_i(k)\ (i \in I_J),\ N'_i(k)\ (i \in I_V),\ 1]^{\mathrm{T}}$ as the control input vector, and for each tunnel segment $i \in I_B$ define the coefficient vector $\boldsymbol{\varphi}_i(k) \in \mathbb{R}^L$ at time interval k as: $\boldsymbol{\varphi}_i(k) = [\alpha_{ij}(k)\ (j \in I_J),\ \beta_{ik}(k)\ (k \in I_V),\ \gamma_i(k)]^{\mathrm{T}}$, where $L = |I_J| + |I_V| + 1$. We make an important modeling choice of function $\boldsymbol{\varphi}_i(k)$ for practical ventilation control: For each $i \in I_B$, $\boldsymbol{\varphi}_i(k)$ depends on k only through traffic intensity $\boldsymbol{\delta}(k)$. This means that function $\boldsymbol{\varphi}_i(\boldsymbol{\delta})$ is time-invariant. Since *Lemma 2* implies $\varphi_{it}(\boldsymbol{\delta}) = \varphi_{it}(\boldsymbol{T}_i \boldsymbol{\delta}_B) = \varphi_{it}(\boldsymbol{\delta}_i)$, we can write $\boldsymbol{\varphi}_i(k) = \boldsymbol{\varphi}_i(\boldsymbol{\delta}_i(k))$. This approach is reasonable given that: 1) traffic is the single major source of disturbance to tunnel airflow: it is the dominant driving force for longitudinal air flow inside the tunnel next to the jet fans; 2) Traffic intensity $\boldsymbol{\delta_B}$ is monitored in the system, and $\boldsymbol{T}_i$ is a time-invariant deterministic linear operator. Historical data for $\boldsymbol{\delta}_i$'s are hence available, For the specified functional form $\boldsymbol{\varphi}_i(\boldsymbol{\delta}_i(k))$, observations of traffic intensity $\boldsymbol{\delta}_i$'s can be used for estimating model coefficients using standard regression techniques; 3) An additive noise term $\varepsilon_i \in \mathbb{R}$ can be introduced to the real underlying system state variable $v_i(k)$, $i \in I_B$ to account for other unmeasured disturbances and modeling errors. Then for control interval k, (4) can be written as:

$$v_i(k) = \boldsymbol{\varphi}_i(\boldsymbol{\delta}_i(k))^{\mathrm{T}} \boldsymbol{u}(k) + \varepsilon_i(k). \qquad i \in I_B \tag{9}$$

We also desire each function $\boldsymbol{\varphi}_i(\boldsymbol{\delta}_i(k))$ ($i \in I_B$) to be calibrated fast for real-time operation. Based on analysis of typical mainline-ramp tunnel system using (2), we find that each $\varphi_{it}(\boldsymbol{\delta}_i)$ ($i \in I_B$) can be well-approximated by an affine function, which implies the follows:

Lemma 3: If we choose $\varphi_{it}(\boldsymbol{\delta}_i)$ to be affine under conditions of *Lemma 2*, then function φ_{it} can be completely specified using only three parameters.

Proof: By the characterization of Π^t in *Lemma 1* and traffic intensity $\boldsymbol{\delta}_i$ defined in *Lemma 2*, we note that for any $i \in I_B \in \Pi^t$, one of the entries in $\boldsymbol{\delta}_i(k) \in \mathbb{R}^3$ can be written as a time-invariant linear combination of the other two. Let $\boldsymbol{\delta}_i'(k)$ represent the other two entries, we can then write $\boldsymbol{\delta}_i(k) = \boldsymbol{T}_i' \boldsymbol{\delta}_i'(k)$, with $\boldsymbol{T}_i' \in \mathbb{R}^{2\times 3}$ with full row rank.

Now assuming the affine function $\varphi_{it}(\boldsymbol{\delta}_i(k)) = \boldsymbol{a}^0{}_{it}{}^{\mathrm{T}} \boldsymbol{\delta}_i(k) + b_{it}$ with $\boldsymbol{a}^0{}_{it} \in \mathbb{R}^3$, and $b_{it} \in \mathbb{R}$, then we have $\varphi_{it}(\boldsymbol{\delta}_i(k)) = \boldsymbol{a}^0{}_{it}{}^{\mathrm{T}} \boldsymbol{T}_i' \boldsymbol{\delta}_i'(k) + b_{it} = \boldsymbol{a}_{it}{}^{\mathrm{T}} \boldsymbol{\delta}_i'(k) + b_{it}$, where $\boldsymbol{a}_{it}{}^{\mathrm{T}} = \boldsymbol{a}^0{}_{it}{}^{\mathrm{T}} \boldsymbol{T}_i'$. Therefore, the triplet $\{a_{it1}, a_{it2}, b_{it}\}$ completely specifies each function $\varphi_{it}(\boldsymbol{\delta}_i)$. ■

Using the notation in the proof of *Lemma 3*, we now re-write (9) to express air flow velocity for each tunnel segment $i \in I_B$ as explicit function of $\boldsymbol{u}$ and $\boldsymbol{\delta}$:

$$\begin{aligned} v_i(k) &= \sum_{t=1}^{l} [\boldsymbol{a}_{it}{}^{\mathrm{T}} \boldsymbol{\delta}_i'(k) + b_{it}] u_t(k) + \varepsilon_i(k) \\ &= \sum_{t=1}^{l} [\boldsymbol{a}_{it}{}^{\mathrm{T}}, b_{it}] \begin{bmatrix} u_t \boldsymbol{\delta}_i'(k) \\ u_t(k) \end{bmatrix} + \varepsilon_i(k) \\ &= \boldsymbol{h}_i(k)^{\mathrm{T}} \boldsymbol{\theta}_i + \varepsilon_i(k), \end{aligned} \tag{10}$$

where $\boldsymbol{h}_i(k) = [u_1(k)\boldsymbol{\delta}_i'(k)^{\mathrm{T}},\ \ldots,\ u_l(k)\boldsymbol{\delta}_i'(k)^{\mathrm{T}},\ \boldsymbol{u}(k)^{\mathrm{T}}]^{\mathrm{T}}$; and $\boldsymbol{\theta}_i = [\boldsymbol{a}_{i1}{}^{\mathrm{T}},\ \ldots,\ \boldsymbol{a}_{il}{}^{\mathrm{T}},\ b_{i1}{}^{\mathrm{T}},\ \ldots,\ b_{il}]^{\mathrm{T}}$. Since $u_l(k) = 1$, (10) is a standard linear model with interaction terms. Model coefficients $\boldsymbol{h}_i(k)$ can be estimated using standard linear regression techniques.

B. Multi-Target Tunnel Ventilation Control

As discussed above, the quantitative relationship between tunnel ventilation control inputs, measured traffic disturbance and system state in one tunnel segment can be approximated using a simple linear model. However, the combined effects of ventilation control inputs across multiple tunnel segments on

air velocity distribution in the system is nontrivial. In addition, tunnel ventilation is required to meet multiple air quality control targets such as limit on maximum CO concentration inside the tunnel and regulation on pollutant discharge rate at tunnel vents/outlets (e.g., maximum allowable NO_x emission rate at every discharge point). Energy efficiency is certainly another consideration in ventilation system design and operations management. This constitutes a multi-input-multi-output (MIMO) problem of distributed parameter system with a centralized control scheme.

The problem can be formulated as an optimization model based on (9) that models the air velocity as a function of input and disturbance, and (5), (6), and (7) that describe pollutant dispersion and discharge. We aim to develop ventilation control strategies (via configuration of ventilation devices including jet fans along the tunnel and axial fans in the vents) to satisfy the multiple air quality control targets/constraints at the minimal energy cost (i.e., minimum number of running fans). Specifically, for a control interval k ($k \geq 1$), the optimization model is given as:

$$\begin{aligned} \min_{\substack{N_i(k),\, i\in I_J \\ N'_i(k),\, i\in I_V}} & \sum_{i\in I_J} N_i(k) + \sum_{i\in I_V} N'_i(k) \\ s.t. \quad & C^{CO}_{\max i}(k) \leq C^{CO}_{\lim}, \ \forall i \in I; \\ & Q^{NO_x}_i(k) \leq Q^{NO_x}_{\lim}, \ \forall i \in \{n\} \cup I_{off} \cup I_{VE}; \\ & N_i(k) \in [N_i^{low}, N_i^{up}], \ \forall i \in I_J; \\ & N'_i(k) \in [N'^{low}_i, N'^{up}_i], \ \forall i \in I_V; \\ & v_i(k) \geq v_i^{low}, \ \forall i \in I; \\ & |N_i(k) - N_i(k-1)| \leq n_{\lim}, \ \forall i \in I_J; \\ & |N'_i(k) - N'_i(k-1)| \leq n'_{\lim}, \ \forall i \in I_V. \end{aligned} \tag{11}$$

In model (11), the objective function is to minimize the total number of running fans (as a surrogate for ventilation energy cost) in all the segments and upper vents. The first two constraints are the maximum CO concentration requirement inside the tunnel and the NO_x emission rate limits at the discharge points, respectively. The next two constraints specify the upper and lower bounds (≥ 0) of control variables (i.e., the number of running fans in each segment and at each upper vent). The v_i^{low} (m/s) in the fifth constraint is the minimum air velocity required in tunnel segment i to ensure enough air exchange rate in the tunnel [19]. Finally, to avoid frequent fan-on/fan-off switches and other abrupt fan adjustments for the saving of fan lifetimes, the last two constraints add limits to the maximum delta changes in the number of running jet-fans and axial fans from one control interval to next.

Note that, (6), (7), (8), and (10) derived earlier are implicitly included in expressing of the first, second and the fifth constraints in terms of the decision variables $\{N_i\ (i \in I_J), N'_i\ (i \in I_V)\}$. This enable us to evaluate how to solve this optimization problem next.

C. Solving the ventilation optimization problem

In the tunnel ventilation optimization model (11) constructed above, the objective function and the last five constraints are linear in terms of decision variables N_i ($i \in I_J$) and N'_i ($i \in I_V$). The first two constraints, when further expanded as functions of the decision variables by plugging in (6)~(8), are nonlinear with respect to N_i ($i \in I_J$) and N'_i ($i \in I_V$) for certain tunnel segments. Specifically, the resulting nonlinear functions are polynomial in terms of N_i or N'_i (or both), with orders ≥ 2 depending on the number of segments upstream the segment in question. Since both N_i and N'_i are integers, the optimization model (11) is a nonlinear integer programing problem.

Remark 2: Note that by taking the negative of its objective function, (11) can be regarded as a convex maximization problem with integer decision variables and polynomial constraints (some polynomials with degree ≥ 2). The model can be further reduced to a linear integer programing if the relevant polynomial constraints are "Integer Convex" [23]. However, this "Integer-Convexity" is hard to verify since both the degree and the coefficients in the relevant polynomials depend on many factors such as the tunnel geometric layout, aerodynamic parameters of the tunnel system. Thus linear integer programing techniques such as cutting plane method or variants of branch and bound method are not suitable for this problem.

Here we propose two practical approaches to solve the optimization problem defined in (11): 1) using the commonly adopted nonlinear programming solution methods such as sequential quadratic programming (SQP) for the continuous relaxation of problem (11), we can then round the resulting optimal solution to their nearest non-negative integers; 2) apply heuristic method such as Tabu search to choose the best solution found to meets all the constraints within given stopping rules. When the total number of running fans required $\{N_i\ (i \in I_J), N'_i\ (i \in I_V)\}$ is relatively small (e.g., $< 10^5$), brute force search can be used provided with acceptable computational cost.

D. Real-Time Ventilation Control

For a control interval k, the algorithm starts by predicting average traffic volume $\hat{\boldsymbol{q}}_B(k) = \{\hat{q}^t_i(k),\ i \in I_B\}$ using time-series models based on traffic monitoring data. Then we recover the complete traffic volume vector prediction:

$$\hat{\boldsymbol{q}}^t(k) = [\hat{\boldsymbol{q}}^t_N(k), \hat{\boldsymbol{q}}^t_B(k)]^{\mathrm{T}} = [-\boldsymbol{A}_N^{-1}\boldsymbol{A}_B\hat{\boldsymbol{q}}^t_B(k), \hat{\boldsymbol{q}}^t_B(k)]^{\mathrm{T}},$$

Where conversion matrix $\boldsymbol{A}$ is defined in *Lemma 1*; $\boldsymbol{A}_B$ consists of the columns in $\boldsymbol{A}$ whose column indices are in I_B; and $\boldsymbol{A}_N$ contains the rest columns in $\boldsymbol{A}$. Next we calculate traffic intensity vector in tunnel segments $\boldsymbol{\delta}_B(k) = \{\ \hat{q}^t_i(k)/q^0_i,\ i \in I_B\}$ using the given base traffic volume data. Finally, we project $\boldsymbol{\delta}_B(k)$ to a lower dimensional $\boldsymbol{\delta}'_i(k) = [\delta_{i1}'(k),\ \delta_{i2}'(k)]^{\mathrm{T}}$ for each tunnel segment $i \in I_B$, both entries of which can be extracted from vector $\boldsymbol{\delta}(k) = \{\ \hat{q}^t_i(k)/q^0_i,\ i \in I\}$.

We summarize the control algorithm and steps for control interval k as below:

a. Predicting tunnel traffic intensity vector $\boldsymbol{\delta}_B(k)$ and calculating the linear mapping of $\boldsymbol{\delta}'_i(k)$ for each tunnel segment $i \in I_B$ using the procedure described above;

b. For each tunnel segment $i \in I_B$, updating model parameters $\alpha_{ik}(k)$, $\beta_{il}(k)$, and $\gamma_i(k)$ (as affine functions of $\boldsymbol{\delta}'_i(k)$) using the predicted $\boldsymbol{\delta}'_i(k)$ and calibrated parameter $\boldsymbol{\theta}_i$;

c. Solving optimization problem (11) for optimal control values of running fans $N_i^*(k)$ ($i \in I_J$), $N'^*_i(k)$ ($i \in I_V$). The control scheme from the previous cycle can be used as the initial iteration vector in solving problem (11);

d. Implementing the resulting control scheme; and then

e. Moving on to next control cycle $k + 1$.

Note that the affine function parameters $\boldsymbol{\theta}_i$ ($i \in I_B$) can also be updated dynamically using the real-time feed of traffic and air quality monitoring data if available. This can be done in either a batch or a recursive fashion.

IV. A Case Study

A. Tunnel Configuration and Simulation Data

For illustration of the ventilation control model developed in this study, the ventilation system of the new Zijingang Tunnel in Hangzhou, China is studied. This 2.16 km-long tunnel underneath Zijingang Rd. has two separate channels with rectangular cross-sections. The two-lane east channel serves the north-bound traffic and the two-lane west channel accommodates the south-bound traffic. Since the east and west channels are physically separate, each channel is essentially an individual tunnel. Here we focus on the east channel that has one on-ramp from Yuhangtang Rd. and one off-ramp to Liuxiang Rd. (Fig. 2). There are two upper vents in the mainline tunnel: one for air supplement and the other for air extraction. Considering the ramp accessing points and the vents, we can divide the tunnel system into $n = 7$ segments: segments 1 to 5 along the direction of traffic are mainline segments; segments 6 and 7 are the on- and off-ramps, respectively. The tunnel is equipped with 49 jet-fans, divided into 16 groups, for north-bound ventilation along the direction of traffic. The segment index sets are $I = \{1, 2, \ldots, 7\}$; $I_{on} = \{6\}$; $I_{off} = \{7\}$; $I_B = \{1, 6, 7\}$; $I_J = I\backslash\{4\}$; $I_V = \{2, 4\}$; $I_{VS} = \{2\}$; $I_{VE} = \{4\}$. More tunnel parameters are given in Table I.

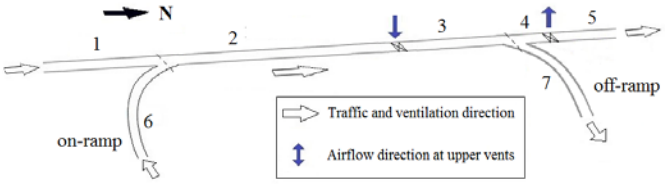

Fig. 2. Layout of the East Channel of Zijingang Tunnel

TABLE I Tunnel Parameters

Notation	Quantity	Value
L_1~L_5	Lengths of mainline segments (km)	0.43, 1.2, 0.35, 0.04, 0.14,
L_6, L_7	Lengths of ramps (km)	0.54, 0.16
S_t, S_r	Cross-section area of mainline, ramps (m^2)	63, 52.5
d_t, d_r	Hydraulic diameter of mainline, ramps (m)	7.875, 7.24
$N^{up}_{1,2,3,5,6,7}$	Available number of jet fans in the segments	9, 20, 10, 2, 6, 2
$N^{low}_{1,2,3,5,6,7}$	Lower bound of number of running jet fans in the segments	0, 0, 0, 0, 0, 0
v_f	Jet speed of the jet fans (m/s)	39
S_f	Cross-section area of a jet fan (m^2)	0.4
K	Pressure-rise coefficient of jet fans	0.88
$N'^{up}_{2,4}$	Number of axial fans available at the air supplement or extraction upper vents	10, -12
$N'^{low}_{2,4}$	Number of axial fans available at the air supplement or extraction upper vents	1, 0
Q_0	Rate flow of each axial fan (m^3/s)	6
$\zeta_{1,2,\ldots,7}$	Local pressure loss coefficient due to curvature, flow convergence or divergence	0.9, 0, 0, 0.1, 1.0, 0.9, 1.3
λ	Tunnel wall friction resistance coefficient	0.02
$q^0_{1,6,7}$	Base traffic volume through mainline entrance, on-ramp and off-ramp (veh/h)	1310, 190, 160
v_t	Average traffic speed (km/h)	40
S_v	Equivalent frontal area of an average vehicle in the tunnel (m^2)	1.5
$n_{\lim}$, $n'_{\lim}$	Delta change limit of fan operations between two adjacent control intervals	6
$v^{low}_{1,2,\ldots,7}$	Minimum required air velocities in tunnel segments (m/s)	2

Vehicular emission factors for CO are estimated according to the baseline emission factor given in [19], and emission factors for NO_x are derived based on [24]. The traffic parameters (e.g., fleet mix, average speed and density) are regarded as homogeneous across tunnel segments, so the emission rates from the tunnel segments are proportional to the lengths of the segments. Using the typical tunnel traffic mix, the composite emission rates of CO and NO_x in the mainline middle sections (segments 2 and 3) are estimated to be 0.22 mg/m/s and 0.003 mg m/s, respectively for baseline free-flow traffic conditions. According to the average local air quality monitoring data [25], the background concentrations for CO and NO_x are C^{CO}_{amb} = 0.72 mg/m^3 and C^{NOx}_{amb} = 0.05 mg/m^3, respectively.

Via tunnel ventilation, we aim to control the maximum CO concentration in the tunnel and NO_x emission rates at the discharge points (e.g., extraction vents and tunnel outlets). According to the PIARC standard [26], The maximum CO concentration in a tunnel is 70ppm (≈ 87.5 mg/m^3 under standard condition). Limits for NO_x emission rates are 120 mg/s and 240 mg/s for extraction vents and tunnel outlet, respectively, according to the air quality control standard regulated by local municipal authority.

From the steady-state pollutant dispersion model (5) for this tunnel, we have $C^{CO}_{\max 2} \geq C^{CO}_{\max 1}$; $C^{CO}_{\max 5} \geq C^{CO}_{\max 4} \geq C^{CO}_{\max 3}$. Therefore, we only need to include constraints on $C^{CO}_{\max 2,\,5,\,7}$ in model (11). Constraints of the NO_x emission rates Q_i^{NOx} at all the three discharge points are included in (11): mainline extraction vent ($i = 4$), mainline outlet ($i = 5$), and off-ramp outlet ($i = 7$). Calculation of these variables is given below:

$$
\begin{aligned}
C^{CO}_{\max 2} &= C^{CO}_{amb} + \frac{A_t(q_1^{CO}L_1 + q_2^{CO}L_2) + A_r q_6^{CO} L_6}{A_t v_2}, \\
C^{CO}_{\max 5} &= C^{CO}_{amb} + \frac{A_t(q_1^{CO}L_1 + q_2^{CO}L_2 + q_3^{CO}L_3) + A_r q_6^{CO} L_6}{A_t v_2 + Q_0 N'_2} + \frac{q_4^{CO}L_4}{v_4} + \frac{q_5^{CO}L_5}{v_5}, \\
C^{CO}_{\max 7} &= C^{CO}_{amb} + \frac{A_t(q_1^{CO}L_1 + q_2^{CO}L_2 + q_3^{CO}L_3) + A_r q_6^{CO} L_6}{A_t v_2 + Q_0 N'_2} + \frac{q_7^{CO}L_7}{v_7}, \\
Q_4^{NO_x} &= \left[C^{NOx}_{amb} + \frac{A_t(q_1^{NO_x}L_1 + q_2^{NO_x}L_2 + q_3^{NO_x}L_3) + A_r q_6^{NO_x} L_6}{A_t v_2 + Q_0 N'_2} + \frac{q_4^{NO_x}L_4}{v_4} \right] Q_0 N'_4, \\
Q_5^{NO_x} &= \left[C^{NOx}_{amb} + \frac{A_t(q_1^{NO_x}L_1 + q_2^{NO_x}L_2 + q_3^{NO_x}L_3) + A_r q_6^{NO_x} L_6}{A_t v_2 + Q_0 N'_2} + \frac{q_4^{NO_x}L_4}{v_4} \right] A_t v_5 + q_5^{NO_x} L_5 A_t, \\
Q_7^{NO_x} &= \left[C^{NOx}_{amb} + \frac{A_t(q_1^{NO_x}L_1 + q_2^{NO_x}L_2 + q_3^{NO_x}L_3) + A_r q_6^{NO_x} L_6}{A_t v_2 + Q_0 N'_2} \right] A_r v_7 + q_7^{NO_x} L_7 A_r.
\end{aligned}
\tag{12}
$$

With (12), we can then construct and solve the optimization problem following (11) for optimal ventilation control of the studied tunnel. Lower and upper bounds of the decision variables are given in Table I.

For illustration, a 4-hour typical traffic scenario (Fig. 3) is used as input for the simulation. With10-minute ventilation control cycle, this translates to $k = 1, 2, \ldots, 24$ control intervals. We assume traffic volume changes in a homogenous pattern, i.e., $\boldsymbol{\delta}_B(k) = \delta(k)\mathbf{1}$ for some $\delta(k) \in \mathbb{R}$, where $\mathbf{1}$ is a vector of one's. The scalar value $\delta(k)$ is profiled in Fig. 3 for the 24 control intervals. In the simulation, every time a new optimal decision is generated, (2) is solved to derive the airflow field in the tunnel. Next (7) and (8) are evaluated to derive system performance (i.e., CO concentrations in the tunnel and NO_x emission rates at the discharge points) from the control scheme. As the initial condition, all the jet-fans are

switched off at the beginning of the simulation. Results from averages over 30 simulations are reported later.

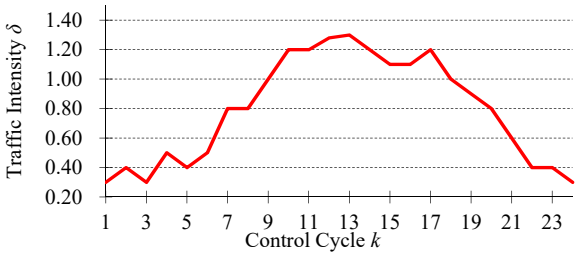

Fig. 3. Traffic intensity profile

B. Calibration of System Parameters

We establish the system of quadratic equations (2) in terms of the steady-state base air flow velocities $\boldsymbol{v}_B = [v_1, v_6, v_7]^T$:

$$\begin{cases} g(v_1) - g(v_6) = 0 \\ f_2(v_1, v_6) + g(v_6) + g(v_7) = 0 \\ f_3(v_1, v_6, v_7) - g(v_7) = 0 \end{cases}, \tag{13}$$

where f_2 and f_3 are quadratic functions of v_1, v_6, and v_7, which are obtained by writing $g_2(v_2) + g_3(v_3)$ in terms of v_1, v_6, and $g_4(v_4) + g_5(v_5)$ in terms of v_1, v_6, and v_7. The calculation of coefficients in the quadratic functions g_i are given in the appendix. Under any given traffic intensity level δ, solving (13) gives us steady-state air velocities v_1, v_6, and v_7 as functions of decision variables $\{N_i\ (i \in I_J), N'_i\ (i \in I_V)\}$. Fig. 4 shows result for the first junction of the tunnel branches under basic traffic volume ($\delta = 1$). One can see the affine relationships between air flow velocities and the decision variables N_i and N'_i, as we rationalized in (3). Interestingly, we also note that $\alpha_{11}, \alpha_{12} > 0$, whereas $\alpha_{16} < 0$, indicating that at for the given traffic intensity condition, enhancing fan operations in a segment tends to speed up airflows in this segment and up- and down-stream serial segments but slow down airflows in its parallel branch segment. This makes air quality control nontrivial in complex tunnels, since increasing the running fans in a segment does not necessarily help pollutant dispersion in other segments.

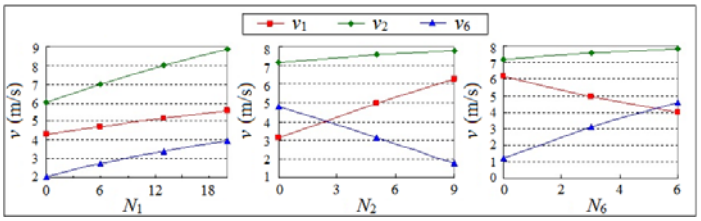

(a) Steady-state relationship between $N_{1,2,6}$ and $v_{1,2,6}$ (δ =1)

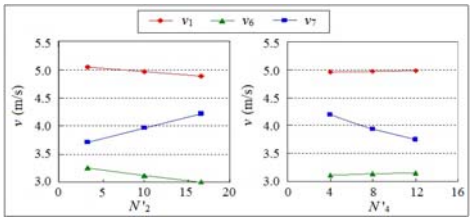

(b) Steady-state relationship between $N'_{2,4}$ and $v_{1,2,6}$ (δ =1)

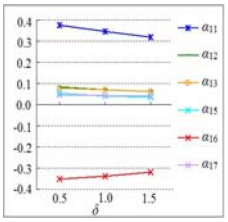

(c) α_{1j} under different δ

Fig. 4. Steady-state airflows in tunnel segments and affine function parameters

In order to quantify the impact of traffic intensity, we calibrate air velocity coefficients $\boldsymbol{\varphi}_{1,6,7}$ using results from cases of δ = 0.5, 1.0, 1.5 (which covers the traffic variation range in tunnel operations). As shown in Fig. 4(c), parameters α_{1k} (k = 1, 2, 3, 5, 6, and 7, the first six entries of $\boldsymbol{\varphi}_1$) are approximately affine in δ, similar pattern is also observed for $\boldsymbol{\varphi}_{6,7}$. The reduced form in (10) is hence justified. Model parameters $\boldsymbol{\theta}_{1,6,7}$ of the affine functions are estimated via linear regression, with results shown in Table II.

TABLE II ESTIMATE OF MODEL PARAMETERS

$\varphi_{ij} = b_{ij} + (a_{ij1} + a_{ij2})\delta$		i = 1		i = 6		i = 7	
		$a_{ij1}+a_{ij2}$	b_{ij}	$a_{ij1}+a_{ij2}$	b_{ij}	$a_{ij1}+a_{ij2}$	b_{ij}
α_{ik}	k = 1	-0.056	0.404	0.388	-0.595	-0.007	0.052
	k = 2	-0.020	0.092	-0.005	0.089	-0.005	0.086
	k = 3	-0.017	0.087	-0.007	0.088	-0.004	0.082
	k = 5	-0.020	0.064	-0.573	0.434	0.053	-0.575
	k = 6	0.033	-0.370	-0.491	0.866	0.001	0.054
	k = 7	-0.006	0.049	0.696	-0.413	-0.065	0.809
β_{ik}	k = 2	0.003	-0.017	0.053	-0.052	0.004	0.034
	k = 4	-0.001	0.005	-0.049	0.037	-0.004	-0.041
γ_i		0.847	2.258	0.199	1.684	0.110	1.906

Note that for each tunnel segment i = 1, 6, 7 and j = 1, 2, …, 8, the sum of $a_{ij1} + a_{ij2}$ is reported instead of a_{ij1}, a_{ij2} separately. This is because we analyze the case of homogenous traffic intensity using a single scalar δ. The two entries of each $\boldsymbol{a}_{ij}^T$ can only be identified by their sum. We can see that as traffic intensity increases, some model parameters increase, while others decrease. This is the result of air flow field interaction, which makes ventilation control nontrivial and demands comprehensive quantitative modeling [4]. We also observe that fan-induced airflow in a tunnel segment is affected mainly by jet-fans in that segment and those in adjacent segments. The effect of fans in segments farther-away diminishes quickly (e.g. see Fig. 4(c)). Similarly, the impact of fan operations in upper vents on tunnel air flows decreases as the tunnel segments are farther away from the vent (see Fig. 4(b)). This provides empirical support to further simplify the parameterization of the reduced form model in (10) if needed.

C. Simulation Results and Discussion

For comparisons, we start by considering only the maximum CO concentration requirement in the tunnel (i.e., applying all the constraints in (11) except for the second one). The resulting ventilation control strategy suggested by solving the model, including N_i ($i \in I_J$), the numbers of running jet-fans, N'_i ($i \in I_V$), the number of axial fans at upper vents, and $\Sigma N_{fi} + \Sigma N'_i$, the total number of running fans, is shown in Fig. 5(a). We can see that the total number of running fans is positively correlated with tunnel traffic. To meet the CO concentration requirement in the tunnel, mainly the jet-fans in the entrance segment 1 and off-ramp segment 7 are operated during high traffic/emission periods. Air extraction fans at the 2nd upper vent are all switched off while only one air supplement fan at 1st upper vent is switched on. The average number of running fans is 7.5 during the high traffic period from t = 80~200 min.

With the suggested optimal ventilation strategy in Fig. 5(a), Figs. 5(b), (c) and (d) depict the resulting longitudinal air velocity in key segments of the tunnel, the maximum CO concentrations in the most polluted tunnel segments (i.e., $C^{CO}_{\max 2,5,7}$), and the NO_x emission rates at all the discharge points ($Q^{NOx}_{4,5,7}$), respectively. Due to the consideration of the $C^{CO}_{\max}$ constraints in designing the ventilation scheme, CO concentrations in the concerned tunnel segments are maintained below the 87.5 mg/m^3 limit throughout the simulation period. There were short instances for control cycles

k = 8 and k = 20 when the maximum CO concentration in the last mainline segment (C^{CO}_{max5}) exceeds the limit slightly (mainly due to traffic prediction error), but the optimal controller reacts quickly to adjust fan operations to the sudden change in traffic to bring CO concentration back under control limit (Fig. 5 (c)). Since the current simulation case neglects NO_x emission constraints at discharge points, the NO_x emission rates at the mainline exit can exceed the municipal standard by as much as 30% during high traffic period (Fig. 5 (d)). On the other hand, there is little NO_x emission discharged at vent 2 since the extraction fans are switched off in this scenario which focus on controlling only CO concentration in the tunnel.

Now taking both maximum CO concentration and NO_x emission rate limits into account, we apply the whole set of constraints in (11). Solving the optimization problem gives us the optimal ventilation strategy (in terms of N_i, N'_i and $\Sigma N_i + \Sigma N'_i$ as shown in Figs. 6(a) and (b), respectively). The total number of operating fans is again positively correlated with traffic/emission, and with much larger number of fans operating in comparison to the previous case where only in-tunnel CO concentration was addressed. In addition to jet fans in segments 1, 2, 7 that were turned on in the previous scenario, ventilation fans in segments 3 and 6 are also switched on to help meet the NO_x emission limits during high traffic period. The specific number of running fans in segment 1 (segment 2) is considerably more (less) than in the previous scenario. Further, to help distribute NO_x emissions across vents for the satisfaction of NO_x discharge limits at the mainline exit, the number of running air extraction fans at upper vent 2 now increases from 0 to an average value of 1.7 during high traffic period t=80 min to 200 min. The air supplement flow at upper vent 1 remains at its lower limit of 6 m^3/s without change. With this ventilation strategy, Figs. 6(c) and (d) show the system performance with respect to $C^{CO}_{max2,5,7}$ and $Q^{NOx}_{4,5,7}$, which are all within the respective limits. Specifically, comparing between the results in Figs.5(c), (d) and those in Figs. 6(d) and (e), we can see that due to the difference in upstream fan operations and air extraction through the 2nd vent, air velocity decreases in the last mainline segment (v_5) while goes up significantly in the off-ramp segment (v_7) compared to the previous case. This helps reduce NO_x emission rate at the mainline exit (Q^{NOx}_5) by increasing NO_x emission rate at off-ramp exit (Q^{NOx}_7) (both below the specified limit of 240 mg/s). Due to more stringent constraints, the average number of running fans increases from 7.5 to 13.08 during the peak traffic (80~200 min), which is 74.4% more than needed when only CO concentration standard is considered.

As such, this study has proposed and demonstrated a multi-target multi-point ventilation control optimization method for complex urban tunnels. The control schemes based on solutions to the nonlinear integer programing problem of tunnel ventilation in response to traffic and emissions are shown effective and energy efficient to comply with in-tunnel air quality requirements as well as emission discharge limits. Aerodynamics and dispersion models in the tunnel are established and calibrated for a serial-parallel tunnel system to capture the fundamental relationships between fan-operations (in the tunnel and at the upper vents) and the airflow velocities, pollutant concentrations, emission discharges. Simulations in

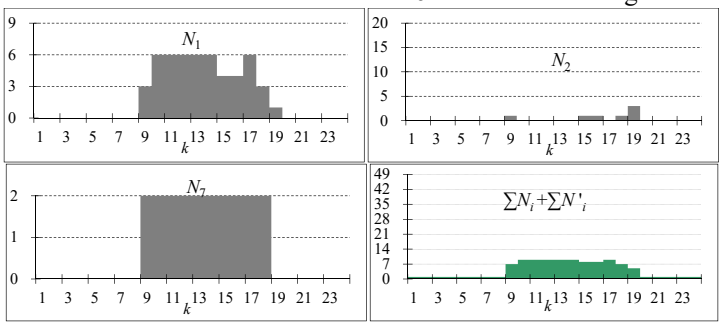

(a) N_i and N'_i sequences and total number of fans operated

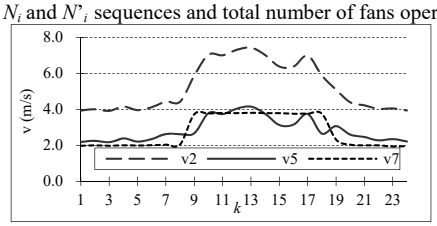

(b) Velocity inside the tunnel

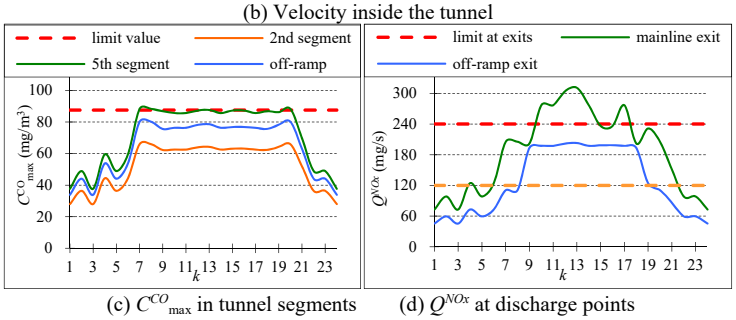

(c) C^{CO}_{max} in tunnel segments (d) Q^{NOx} at discharge points

Fig. 5. Tunnel ventilation control (with C^{CO}_{lim} requirements)

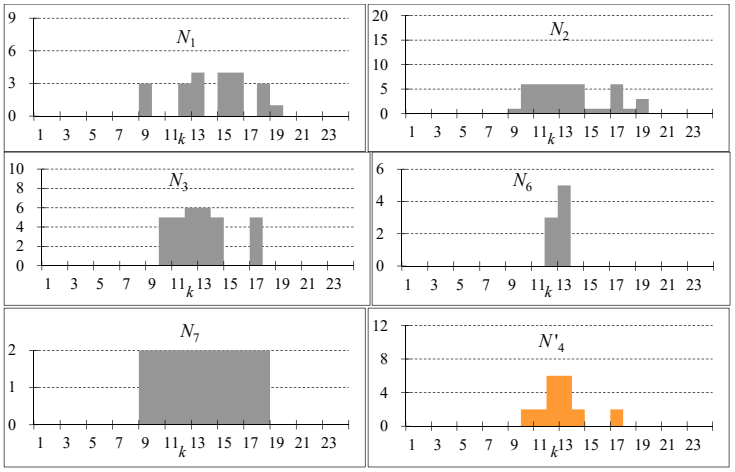

(a) N_i and N'_i sequences for ventilation control

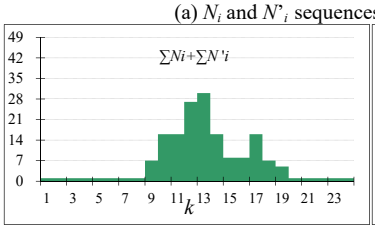

(b) The total number of fans on

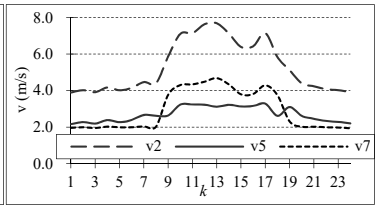

(c) Velocity inside the tunnel

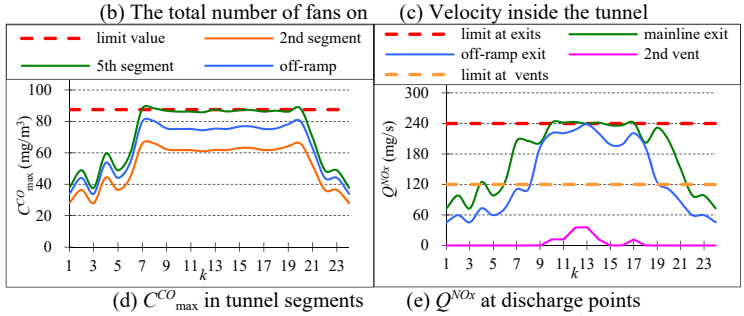

(d) C^{CO}_{max} in tunnel segments (e) Q^{NOx} at discharge points

Fig. 6. Tunnel ventilation control (with both C^{CO}_{lim} and Q^{NOx}_{lim} targets)

the case study demonstrate the effectiveness of the proposed method, which can be adopted in tunnel ventilation design and operations to calculate special proportions and sequences of the running fans in different tunnel segments and upper vents in order to meet multiple control requirements.

For implementation in real world applications, we will also need to account for possible time-varying parameters due to unmeasured disturbances. This can be done by adaptively tuning model parameters γ_i (or the hyper-parameters $\boldsymbol{a}_{il}$ and b_{il} associated with it). More sophisticated traffic prediction models can also be incorporated. Other factors such as spatial variation of traffic flow in the tunnel and better resolved vehicle emission factors can be used. The modeling framework can also be expanded for two-way traffic tunnels. For more advanced variable jet-fan speed control, dynamic traffic and aerodynamics models can be used for shorter control intervals to adjust fan speed in addition to number of operating fans.

APPENDIX

In this Appendix, we provide a detailed description of aerodynamics modeling steps for general mainline-ramp structured complex tunnels.

Step 1. Force Balance in Each Tunnel Segment

The steady state force balance equation (A1) below holds for air flow in each tunnel segment:

$$\sum F = F_t + F_f + F_r + F_e = 0, \tag{A1}$$

where ΣF is the sum of the external forces (kN) imposed on the air in the segment, which consists of four parts [19][27] [28]:

a. F_t is the ventilation force due to traffic:

$$\begin{aligned} F_t &= \frac{\rho}{2}\sum_{k=1}^{M} C_{dk} S_{vk} (v_{vk} - v) \,|\, v_{vk} - v \,| \\ &= \frac{\rho}{2}\frac{\delta q^0 L}{v_t} S_v (v_t - v) \,|\, v_t - v \,|, \end{aligned} \tag{A1a}$$

where ρ is the air density (kg/m^3); v is the longitudinal air velocity (m/s); v_t is the average speed of the vehicles (m/s); $M = \delta q^0 L/v_t$ is the total number of vehicles in the tunnel segment; L is the segment length (m); S_{vk} is the frontal area of vehicle k (m^2), v_{vk} is the speed of vehicle k (m/s); C_{dk} is the drag coefficient of vehicle k; $S_v = \Sigma_k C_{dk} S_{vk}/M$ is the equivalent frontal area of an average vehicle in the segment.

b. F_f is the ventilation force by jet-fans in operation:

$$F_f = N\rho K S_f v_f (v_f - v), \tag{A1b}$$

where N is the number of running jet-fans in the segment, K is the pressure-rise coefficient depending on the specification parameters of jet-fans [26], S_f is the cross-sectional area of the jet fan (m^2), v_f is the jet speed through the jet-fans (m/s).

c. F_r is the frictional resistance and local pressure loss:

$$F_r = -\frac{\rho}{2} S \left(\lambda \frac{L}{d_e} + \zeta\right) v^2, \tag{A1c}$$

where S is the cross-sectional area of the tunnel segment (m^2), λ is the friction resistance coefficient of the tunnel wall, d_e is the hydraulic diameter of the tunnel segment (m), ζ is the coefficient of local pressure loss [29].

d. F_e is the force of the boundary pressure difference:

$$F_e = S(p_{\text{in}} - p_{\text{out}}), \tag{A1d}$$

where p_{in} and p_{out} are the static pressure (kPa) at the starting and ending points of the segment, respectively.

Step 2. Eliminating Segments' Boundary Pressure Variables

Applying (A1) to all the tunnel segments $i \in I$, we have

$$\begin{cases} g_i(v_i) - p_i/\rho = 0, \ (i = 1), \\ g_i(v_i) + p_{i-1}/\rho - p_i/\rho = 0, \ (i = 2,\ldots,n-1), \\ g_i(v_i) + p_{i-1}/\rho = 0, \ (i = n), \\ g_i(v_i) - p_j/\rho = 0, \ (i \in I_{\text{on}}, j = h_i), \\ g_i(v_i) + p_j/\rho = 0, \ (i \in I_{\text{off}}, j = h_i), \end{cases} \tag{A2}$$

where quadratic function $g_i(v_i) = a_i v_i^2 + b_i v_i + c_i$, with coefficients given below (in a_i, b_i, c_i, the subscript i is omitted for variables that are constant across different segments):

$$\begin{aligned} a_i &= \frac{\delta q_i^0 L_i S_{vi}}{2 S_i v_{ti}} - \frac{\lambda L_i}{2 d_{ei}} - \frac{\zeta_i}{2}, \ b_i = -\frac{N_i S_f K v_f + \delta q_i^0 L_i S_{vi}}{S_i}, \\ c_i &= \frac{2 N_i S_f K v_f^2 + \delta q_i^0 L_i S_{vi} v_{ti}}{2 S_i}, \ \forall i \in I, \end{aligned} \tag{A3}$$

p_i in (A2) is the static pressure at the exit of segment i, i.e., it is p_{out} for segment i and p_{in} for segment $i + 1$.

In the model, we assume that the static pressure at tunnel portals is zero, in particular $p_0 = p_n = 0$. So we have $|I| = n + m$ independent equations in (A2) with $n+m$ unknown velocity variables and $n - 1$ unknown segment boundary pressure variables. Apparently, we can eliminate them as below:

(i) For $i = h_j$ with $j \in I_{on}$ we write $p_i = g_j(v_j)$, and for $i = h_j$ with $j \in I_{off}$ we write $p_i = -g_j(v_j)$, this is based on the last two equations in (A3) that encode the "*pressure balance*" condition;

(ii) For all adjacent pairs of two ramps j and j' ($n < j < j'$), do the following: if there are some segments between segment h_j and $h_{j'}$ ($n < j < j'$) i's, then combining the first equation in (A2) over $\{i: h_{j'} \geq i > h_j\}$, we have:

$$p_{h_j} - p_{h_{j'}} + \sum_{i=h_j+1}^{h_{j'}} g_i(v_i) = 0. \tag{A4a}$$

(iii) Combine the first equation in (A2) over $\{i: h_{n+1} \geq i \geq 1\}$, and sum over $\{i: n \geq i > h_{n+m}\}$, we get:

$$\begin{cases} -p_{h_{n+1}} + \sum_{i=1}^{h_{n+1}} g_i(v_i) = 0, \\ p_{h_{n+m}} + \sum_{i=h_{n+m}+1}^{n} g_i(v_i) = 0. \end{cases} \tag{A4b}$$

(iv) Use the results obtained from (i) to eliminate the boundary pressure terms in (A4).

After steps (i)~(iv), the $n - 1$ segments' boundary pressure variables are all eliminated, what remains is a system of $(n + m) - (n - 1) = m + 1$ equations of $n + m$ air velocity variables:

$$\begin{cases} \pm g_{n+1}(v_{n+1}) + \sum_{i=1}^{h_{n+1}} g_i(v_i) = 0, \\ \pm g_{n+1}(v_{n+1}) \pm g_{n+2}(v_{n+2}) + \sum_{i=h_{n+1}+1}^{h_{n+2}} g_i(v_i) = 0, \\ \quad \vdots \\ \pm g_{n+m-1}(v_{n+m-1}) \pm g_{n+m}(v_{n+m}) + \sum_{i=h_{n+m-1}+1}^{h_{n+m}} g_i(v_i) = 0, \\ \pm g_{n+m}(v_{n+m}) + \sum_{i=h_{n+m}+1}^{n} g_i(v_i) = 0. \end{cases} \tag{A5}$$

In the last equation the sign in front of the $g_{n+j}(v_{n+j})$ term is positive if $n + j \in I_{on}$ and negative otherwise (i.e., $n + j \in I_{off}$); in

each of the other equations the sign in front of the $g_{n+j}(v_{n+j})$ term that is beside the summation is negative if $n + j \in I_{on}$ and positive otherwise (i.e., $n + j \in I_{off}$); the sign in front of any other $g_{n+j}(v_{n+j})$ term is positive if $n + j \in I_{on}$ and negative otherwise.

Step 3. Eliminating Non-Basic Air Velocity Variables

Based on the definition of I_B and the proof of *Lemma* 1, we partition $\boldsymbol{v} = [\boldsymbol{v}_B{}^{\mathrm{T}}, \boldsymbol{v}_N{}^{\mathrm{T}}]^{\mathrm{T}}$ in accordance to $\boldsymbol{q}^a = [\boldsymbol{q}^a{}_B{}^{\mathrm{T}}, \boldsymbol{q}^a{}_N{}^{\mathrm{T}}]^{\mathrm{T}}$. Since for each $i \in I$, $v_i = q^a{}_i/S_i$, we can write:

$$\boldsymbol{v}_N = \boldsymbol{D}_N^{-1}\boldsymbol{q}_N^a = \boldsymbol{D}_N^{-1}\boldsymbol{A}_N^{-1}(\boldsymbol{b} - \boldsymbol{A}_B\boldsymbol{q}_B^a) = \boldsymbol{D}_N^{-1}\boldsymbol{A}_N^{-1}(\boldsymbol{b} - \boldsymbol{A}_B\boldsymbol{D}_B\boldsymbol{v}_B),$$

where $\boldsymbol{D}_N \in \mathbb{R}^{(n-1)\times(n-1)}$ is a diagonal matrix that has its j th diagonal entry $d_{jj} = S_i$, v_i corresponds to the j^{th} entry of $\boldsymbol{v}_N$; $\boldsymbol{D}_B \in \mathbb{R}^{(m+1)\times(m+1)}$ is a diagonal matrix that has its j^{th} diagonal entry $d_{jj} = S_i$, and v_i corresponds to the j^{th} entry of $\boldsymbol{v}_B$.

Let $\boldsymbol{H} = [\boldsymbol{I} \;\; (-\boldsymbol{D}_N{}^{-1}\boldsymbol{A}_N{}^{-1}\boldsymbol{A}_B\boldsymbol{D}_B)^{\mathrm{T}}]^{\mathrm{T}}$ and $\boldsymbol{s} = [\boldsymbol{0}^{\mathrm{T}} \;\; (\boldsymbol{D}_N{}^{-1}\boldsymbol{A}_N{}^{-1}\boldsymbol{b})^{\mathrm{T}}]^{\mathrm{T}}$, so we can write $\boldsymbol{v} = [\boldsymbol{v}_B{}^{\mathrm{T}}, \boldsymbol{v}_N{}^{\mathrm{T}}]^{\mathrm{T}} = \boldsymbol{H}\boldsymbol{v}_B + \boldsymbol{s}$. Then the k^{th} equation in (A5) can be expressed as:

$$(\boldsymbol{H}\boldsymbol{v}_B + \boldsymbol{s})^{\mathrm{T}}\boldsymbol{D}_k(\boldsymbol{H}\boldsymbol{v}_B + \boldsymbol{s}) + \boldsymbol{r}_k^{\mathrm{T}}(\boldsymbol{H}\boldsymbol{v}_B + \boldsymbol{s}) + z_k = 0,$$

where $\boldsymbol{D}_k \in \mathbb{R}^{(n+m)\times(n+m)}$ is a diagonal matrix, $\boldsymbol{r}_k \in \mathbb{R}^{(n+m)}$, $z_k \in \mathbb{R}$. If $g_i(v_i)$ is present in the k^{th} equation of (A5) and v_i corresponds to j^{th} entry in vector $[\boldsymbol{v}_B{}^{\mathrm{T}}, \boldsymbol{v}_N{}^{\mathrm{T}}]^{\mathrm{T}}$, then the j^{th} diagonal entry of $\boldsymbol{D}_k$ is $\pm a_i$ and the j^{th} entry of $\boldsymbol{r}_k$ is $\pm b_i$ (the rule of setting the sign is the same as that in (A5)), otherwise these entries in $\boldsymbol{D}_k$ and $\boldsymbol{r}_k$ are zero. z_k is the sum of the rest constant terms (i.e., $\pm c_i$'s) in the k^{th} equation of (A5).

Now if we define for $k = 1, \ldots, m + 1$:

$$\begin{cases} \boldsymbol{\Lambda}_k = \boldsymbol{H}^{\mathrm{T}}\boldsymbol{D}_k\boldsymbol{H} \\ \boldsymbol{\eta}_k = \boldsymbol{H}^{\mathrm{T}}(2\boldsymbol{D}_k\boldsymbol{s} + \boldsymbol{r}_k) \\ \omega_k = (\boldsymbol{s}^{\mathrm{T}}\boldsymbol{D}_k + \boldsymbol{r}_k^{\mathrm{T}})\boldsymbol{s} + z_k \end{cases}, \tag{A6}$$

then it follows that we can write system (A5) in the form of (1) in the main text.

REFERENCES

[1] W. Broere, "Urban underground space: Solving the problems of today's cities," *Tunn. and Und. Space Tech.*, vol. 55, pp. 245-248, May. 2016.

[2] T. Du, D. Yang, S. Peng and Y. Xiao, "A method for design of smoke control of urban traffic link tunnel (UTLT) using longitudinal ventilation," *Tunn. and Und. Space Tech.*, vol. 48, pp. 35-42, Apr. 2015.

[3] Y. Chen, "Discussion of calculation method for multiple-ramp ventilation systems in urban highway tunnels," *Modern Tunn. Tech.*, vol. 48, no. 5, pp. 97-100, May 2011.

[4] F. Xi, "Ventilation mode design of Wuxi Taihu Avenue Tunnel," *Und. Eng. and Tunn.* (in Chinese), vol. 3, no. 1, pp. 29-31, 2011.

[5] W. Chow, M. Chan, "Field Measurement on Transient Carbon Monoxide Levels in Vehicular Tunnels," *Building and Environment*, vol. 38, no. 2, pp. 227-236, Feb. 2003.

[6] S. Bogdan, B. Birgmajer, "Model Predictive Fuzzy Control of Longitudinal Ventilation system in a Road Tunnel," Trans. Res. Part C, vol. 16, no. 5, Oct. 2008.

[7] P. Chen, J. Lai, C. Lin, "Application of fuzzy control to a road tunnel ventilation system," *Fuzzy Sets and Systems*, vol. 100, no. 1-3, pp. 9-28. Nov. 1998.

[8] H. Jozef, S. Juraj.; Š. Vojtech, "Process Model and Implementation the Multivariable Model Predictive Control to Ventilation System," in *Proc. of SAMI 8th IEEE Inter. Sym. on App. Mach. Intel. and Inform.*, Herlany, Slovakia, Jan. 2010, pp. 211-214.

[9] Y. Zhang and W. Jin, "A Road Tunnel Longitudinal Ventilation Control System Based on Fuzzy-Neural Network," in *Proc. of the 5th World Cong. on Intel. Con.and Aut.*, Jun. 2004, pp. 3570-3574.

[10] B. Chu, D. Hong, J. Park, "Tunnel ventilation control via an actor-critic algorithm employing nonparametric policy gradients," *Journal of Mech. Sci.and Tech.*, vol. 23, no. 2, pp. 311-323, Feb. 2009.

[11] Z. Tan, Z. Huang, K. Wu, L. Xu, "Simulation Analysis of Longitudinal Ventilation System with Jet-fan Speed Control for MPC strategy in a Road Tunnel," in *Proc. of 15th IEEE Intel. Trans. Sys. Conf.*, Sep. 2012, pp. 1271-1276.

[12] C. Hu, "Study of natural ventilation of urban tunnel with upper vents," M.S. thesis, Dept. Mech. Eng., Southwest Jiaotong Univ., Chengdu, China, 2005.

[13] J. Ling, H. Hao, J. Li, J. Xing and X. Zheng, "Numerical simulation of natural ventilation in city road tunnel with upper vents," in *Proc. of 2011 Inter. Conf. on Elect. Tech. and Civil Eng.*, Apr. 2011, pp. 5227-5230.

[14] S. Mao, D. Yang., "One-dimensional analysis for optimizing smoke venting in tunnels by combining roof vents and longitudinal ventilation," *App. Ther. Eng.*, in press, available on-line, Aug. 2016.

[15] L. Ferkl and G. Meinsma, "Finding optimal ventilation control for highway tunnels," *Tunn. and Und. Space Tech.*, vol. 22, no. 2, pp. 222-229, Mar. 2007.

[16] L. Ferkl, M. Gjerrit and Š. Michael, "A linear Programming Approach for Ventilation Control in Tunnels," in *Pro. of the 45th IEEE Conf. on Dec.& Cont.*, San Diego, CA, USA, pp. 6672-6677, Dec. 2006.

[17] US DOT (1997). Subway environmental design handbook, vol. II, Subway environmental simulation computer program, Version 4, Part 1, User's manual.

[18] Tan, Z. and H. Gao (2017). "Optimizing vents layout and configuration of complex urban tunnels for air quality control," *IEEE Trans. on Contr. Sys. Tech*., vol. PP, no. 99, 1-9, Jan. 2017, available on line.

[19] Chinese DOT (2000). Specifications for Design of Ventilation and Lighting of Highway Tunnel (JTJ026.1-99).

[20] Z. Tan, Y. Xia, Q. Yang and G. Zhou, "Adaptive fine pollutant discharge control for motor vehicles tunnels under traffic state transition," *IET Intel. Trans. Sys.*, vol. 9, no. 8, Oct. 2015.

[21] Tan, Z. Study on inertia effect and linkage control of urban tunnel ventilation. M.S. Dissertation, Zhejiang University, Hangzhou, China, 2013.

[22] M. EL-Fadel and Z. Hashisho, "Vehicular emissions and air quality assessment in roadway tunnels: the Salim Slam tunnel," *Trans. Res. Part D*, vol. 5, no. 5, pp. 355-372, May 2000.

[23] R. Hemmecke, M. Köppe, J. Lee, and R. Weismantel, "Nonlinear Integer Programming", in *50 Years of Integer Programming 1958-2008: The Early Years and State-of-the-Art Surveys*, Berlin, Germany: Springer-Verlag, 2009, ch. 15, sec. 2.

[24] State Environmental Protection Administration of China (2005). Light vehicle emission limits and measurement methods (China III, IV stage).

[25] Zhejiang Hangzhou Air Quality Index (website). Hangzhou, China, accessed Apr. 2015: http://www.tianqi.com/air/hangzhou.html

[26] PIARC Technical Committee C.4 Road Tunnel (2012). Road tunnels: vehicle emissions and air demand for ventilation. PIARC, Paris, France.

[27] A. Martegani, G. Pavesi and C. Barbetta, "The influence of separation, inclination and swirl on single and coupled jet fans installation efficiency," in *Proc. of the 9th Inter. Sym. on Aero. and Vent. of Veh. Tunn.*, Oct. 1997, pp. 43-55.

[28] H. Jang and F. Chen, "On the determination of the aerodynamic coefficients of highway tunnels," *Journal of Wind Engineering and Industrial Aerodynamics*, vol. 90, no. 8, pp. 869-896, Aug. 2002.

[29] L. Kurka, L. Ferkl, O. Sladek, and J. Porizek, "Simulation of traffic, ventilation and exhaust in a complex road tunnel," in *Proc. of IFAC*, Jan. 2005, pp. 2032-2032.